RSC Advances

PAPER

View Article Online
View Journal | View Issue

Check for updates

Cite this: *RSC Adv.*, 2019, **9**, 17691

Preparation and application of solid-state upconversion materials based on sodium polyacrylate†

Changqing Ye, Jinsuo Ma, Pengju Han,* Shuoran Chen, Ping Ding, Bin Sun and Xiaomei Wang*

By loading a microemulsion containing both sensitizer and emitter into porous sodium polyacrylate (PAAS), a water-absorbent resin (WAR) upconversion (UC) material was fabricated for photocatalysis applications. This WAR UC material showed a highly efficient UC process in the ambient environment owing to its liquid/solid encapsulation structure. In the application measurement, the UC emission from WAR UC materials can excite the catalyst Pt/WO_3 to produce hydroxyl radicals, yielding 7-hydroxycoumarin by reacting with coumarin. In another case, since the band gap of ZnCdS matches the energy of UC emission, hole–electron pairs can be obtained under the UC irradiation and capture electrons from rhodamine B, leading to the degradation of rhodamine B. The maximum of the photocatalysis efficiency can be up to 97%. This work solves the oxygen quenching problem by preparing a triplet–triplet annihilation upconversion (TTA-UC) O/W microemulsion and loading it into PAAS WAR, and opens a new avenue to solid-state devices for TTA-UC. The applications of photocatalytic synthesis and photocatalytic degradation lay a foundation for future practical applications for TTA-UC materials.

Received 8th February 2019
Accepted 18th May 2019

DOI: 10.1039/c9ra01027k

rsc.li/rsc-advances

Open Access Article. Published on 05 June 2019. Downloaded on 12/9/2025 5:39:30 PM.
This article is licensed under a Creative Commons Attribution-NonCommercial 3.0 Unported Licence.

1 Introduction

Upconversion is a phenomenon of lower-energy (longer wavelength) photons converted into higher-energy photons (shorter wavelength), which can be carried out by either two-photon absorption excited by the illuminant with high power density[1–3] or triplet–triplet annihilation (TTA) excited with low power density.[4–7] Owing to the potential widespread practical applications such as in photovoltaics,[8,9] photocatalysis[10,11]/photodegradation,[12,13] photodynamic therapy of cancer[14,15] and displays,[16] triplet–triplet annihilation upconversion (TTA-UC) has attracted more attention.

A TTA-UC system mainly consists of a triplet sensitizer and annihilator,[17–19] and the UC mechanism can be divided into several micro-channel processes as follows:[20–22] Upon excitation of the low-energy illuminant, the triplet sensitizer will achieve its singlet state ($^1S^*$), followed by an intersystem crossing process to reach the triplet state ($^3S^*$). Secondly, the energy will be transferred to the annihilator to generate its triplet state ($^3A^*$) *via* triplet–triplet energy transfer. Thirdly, two triplet state annihilator will further annihilate by collision and populate the singlet-excited state. This annihilator at the singlet-excited state could ultimately go back to the ground state with UC fluorescence.[23]

Researches of TTA-UC material were generally carried on within solution system ever since proposed in 1962.[24] Moreover, the mechanism of TTA-UC is based on the triplet population, triplet energy transfer and triplet annihilation process of organic compounds, so the system should be isolated from oxygen to avoid the quenching of triplet excitons.[25–27] Inevitably, necessity of anaerobic environment and solution system significantly restricts the practical application of TTA-UC.[28] Thus, high-efficiency TTA-UC in the ambient environment has attracted great interest and been explored by many researchers. For example, sensitizers and annihilators were embedded into solid polymer films[29,30] or nano particles,[31] including ethyleneoxide–epichlorohydrin copolymer[32] with low glass transition temperature or rigid polymethyl methacrylate.[33] The encapsulation of sensitizers and annihilators could produce anaerobic environment for TTA-UC. However, the triplet–triplet energy transfer and TTA processes of TTA-UC were somewhat suffocated as the diffusion of sensitizers and annihilators restricted by polymer encapsulation and in consequence leading to the significantly decreased quantum efficiency.[34,35] So, compared with organic solvents system, these strategies all involved complex preparation process and low UC efficiency,[36] which made TTA-UC difficult for further applications.

For above concerns, we explored a new liquid/solid encapsulation strategy for developing high TTA-UC system. First, we

Research Centre for Green Printing Nanophotonic Materials, Jiangsu Key Laboratory for Environmental Functional Materials, Institute of Chemistry, Biology and Materials Engineering, Suzhou University of Science and Technology, Suzhou 215009, P. R. China. E-mail: wxyhpj@163.com

† Electronic supplementary information (ESI) available. See DOI: 10.1039/c9ra01027k

Open Access Article. Published on 05 June 2019. Downloaded on 12/9/2025 5:39:30 PM.
This article is licensed under a Creative Commons Attribution-NonCommercial 3.0 Unported Licence.

utilized an o/w microemulsion which can act as an effective medium for TTA-UC performance in ambient air environment to dissolve the sensitizer PdTPP and the annihilator DPA. Then the O/W microemulsion was further encapsulated into a water-absorbent resin (WAR) of the porous sodium polyacrylate (PAAS) to fabricate solid-state UC material, which can realized highly efficient solid-state TTA-UC in practical ambient environment. This WAR solid-state UC material has been demonstrated to be applied in photocatalytic synthesis of 7-hydroxycoumarin and photocatalytic degradation of rhodamine B, which could lay a foundation for future practical effective energy utilization applications for TTA-UC materials.

2 Experimental section

2.1 Materials

Palladium(II) tetraphenylporphyrin (PdTPP) was synthesized as previously reported.[5] Acrylic acid, sodium hydrate, isopropyl alcohol, potassium peroxodisulfate and toluene were purchased from Tianjin Bodi Chemical co. Tween-20, 9,10-diphenylanthracene (DPA), $H_2PtCl_6 \cdot H_2O$ and nano powder WO_3 were purchased from J&K Chemical technology co. Methanol, coumarin and ethyl alcohol were purchased from Sinopharm Reagent Co. All reagents were analytical reagents and used as received without further purification. Deionized water was used in the experiments throughout.

2.2 Preparation of WAR UC materials

An amount of 36 mL deionized water was added into a 150 mL three-necked flask, and the flask was then bubbling nitrogen by a N_2-vent needle for 40 min. 10 mL Tween-20 was then added into the flask with syringe and dissolved in deionized water with magnetic stirring. After that, 4 mL mixed toluene solution contained PdTPP (0.12 mM) and DPA (36 mM) was added into the flask with syringe. The mixed solution was magnetic stirred under nitrogen atmosphere to form a homogeneous microemulsion. The microemulsion was static down to transparency and sealed for further experiment.

PAAS WAR was prepared using acrylic acid as the monomer and potassium persulfate as the initiator. 8 g NaOH and 20 mL deionized water was added into a 250 mL three-necked flask. When the NaOH was dissolved with magnetic stirring and the solution cool down, 25 mL acrylic acid was slowly added in with magnetic stirring in cold bath. Then 20 mL isopropyl alcohol was added in and the solution was transferred to a water bath of 70 °C. After that, 5 mL potassium peroxodisulfate (40 mM) was dropwise added through dropping funnel with constant pressure. After becoming viscous, the solution was transferred into a 150 mL beaker and the reaction continued in a constant temperature oven of 50 °C for 2 h. As the polymerization finished, raw PAAS was obtained as a faint yellow solid. Before applied in the next section, PAAS solid was immersed in ethyl alcohol for 2 h and then dried, placed in drying oven for further experiment.

10 g dried PAAS was put into the prepared UC O/W microemulsion and soaked for about 48 h. The whole process was operated in a glovebox and the quantity of water and oxygen were both below 10 ppm. After the microemulsion was well adsorbed, the surface of PAAS WAR UC materials was dried by nitrogen flow and then kept in atmospheric environment before further tests and applications.

2.3 Upconversion property measurements

Excitation source for UC was a solid-state continuous laser (Nd:YVO_4 + KTP) with wavenumber of 532 nm and power density of 60 mW cm^{-2}. First, a mount of mixed toluene solution contains PdTPP (0.12 mM) and DPA (36 mM) was put into a quartz colorimetric ware and bubbling nitrogen by a N_2-vent needle for 40 min. Then the green laser (532 nm, 60 mW cm^{-2}) irradiated at the solution in the quartz colorimetric ware and the blue upconverted fluorescence appeared.[37] Spectrum of the UC fluorescence was recorded by spectral scanning colorimeter (PR-655) with a 532 nm optical filter to get rid of the scattered laser peak.

2.4 Photocatalytic synthesis experiment driven by WAR UC materials

Preparation of photocatalyst Pt/WO_3 was as follows: 130 mg WO_3 nano powder, 30 mL deionized water and 10 mL methanol were put in a 100 mL beaker with ultrasonic treated for 30 min. Then $H_2PtCl_6 \cdot H_2O$ (0.4 mL, 5×10^{-2} mol L^{-1}) was added in the beaker with stirring. After evenly stirred, the beaker was packaged by foil, irradiated under mercury lamp (500 W). The obtained solid was then filtered, washed with deionized water and absolute ethyl alcohol, dried and compounded as aqueous solution (10 g L^{-1}) for further experiment.

Application demonstration of photocatalytic synthesis driven by WAR UC materials was as follows. 5 mL coumarin aqueous solution (200 mg L^{-1}), 0.6 mL prepared photocatalyst Pt/WO_3 (10 g L^{-1}) were stirred evenly in a 100 mL beaker, and then 1.5 g WAR UC materials was taken in the mixed solution. Green laser (532 nm, 60 mW cm^{-2}) irradiated directly at WAR UC materials and the obtained blue UC fluorescence could irradiate at coumarin aqueous solution consequently. The beaker was also packaged by foil to reduce the loss of UC fluorescence. The solution was extracted every 20 min to detect the fluorescence spectrum of 7-hydroxycoumarin. All the experiments were carried out in ambient environment.

2.5 Photocatalytic degradation experiment driven by PAAS WAR UC materials

ZnCdS powder was used as the photocatalyst candidates since its absorption edges at 528–573 nm and the estimated band-gaps at 2.35–2.17 eV that could effectively absorb our green-to-blue upconversion (436 nm, 2.84 eV) to form electron/hole (e^-/h^+) pairs,[38] which made it be able to degrade rhodamine B.

Application demonstration of photocatalytic degradation driven by WAR UC materials was as follows: 5 mL rhodamine B aqueous solution (10 μM), 25 mg ZnCdS powder were stirred evenly in a 100 mL beaker, and then 1.5 g WAR UC materials was taken in the mixed solution. Green laser (532 nm, 60 mW cm^{-2}) irradiated directly at WAR UC materials and the obtained blue

 This journal is © The Royal Society of Chemistry 2019

Open Access Article. Published on 05 June 2019. Downloaded on 12/9/2025 5:39:30 PM.
This article is licensed under a Creative Commons Attribution-NonCommercial 3.0 Unported Licence.

UC fluorescence could irradiate at rhodamine B aqueous solution consequently. The beaker was also packaged by foil to reduce the loss of UC fluorescence. The solution was extracted every 20 min to detect the absorption fluorescence spectra of rhodamine B. All the experiments were carried out in ambient environment.

3 Results and discussion

In this paper, PdTPP was used as the sensitizer and DPA as the annihilator to constitute TTA-UC system. As metalloporphyrin complex, PdTPP showed a Soret absorption band at 415 nm and a Q-band at 510–550 nm (Fig. 1a), which determined the wavelength of the exciting laser (532 nm). There were two emission characteristic peaks as the fluorescence at 610 nm and phosphorescence at 710 nm, respectively (Fig. 1a).

Absorption of DPA appeared respectively at 324 nm, 341 nm, 359 nm and 378 nm that belonged to the vibration of anthracene group of DPA (Fig. 1b). Excited by laser of 532 nm, emission characteristic peak showed at 400–450 nm, which revealed DPA was an appropriate luminescent material.

The preparation process of PAAS WAR is as follows. Firstly, sodium acrylate was prepared through neutralization reaction of acrylic acid and sodium hydroxide. Secondly, sodium acrylate monomers combined with free radicals that obtained by thermal decomposition of the initiator potassium peroxodisulfate to realize chain growth. Thirdly, isopropyl alcohol was added as chain transfer agent while PAAS grew into long chain macromolecular polymer. The prepared PAAS resin was faint yellow solid gel (Fig. 2a). As shown in SEM image (Fig. 2b), porous microstructures can be seen bestrewed within the PAAS resin, which made PAAS WAR excellent absorption performance. The water absorbency was 400 mL g^{-1} (eqn (S8), ESI†). Therefore, the microemulsion can be absorbed into PAAS resin to form WAR UC materials.

Micro-droplets of PdTPP/DPA/toluene homogeneously dispersed in PAAS resin along with O/W microemulsion as seen in Fig. 2d. PdTPP and DPA molecules can move unrestrictedly as in solution system, which made the energy transfer smoothly as seen in Fig. 2c. Excited by laser of 532 nm, there revealed obvious blue light path in WAR material, which showed a high efficiency as in solution system with anaerobic treatment. All the experiments were carried out in the ambient environment, which revealed that WAR UC materials had solved the problems of oxygen-quenching and low UC efficiency in solid-state system.

Absorption and emission properties of PAAS matrix in range of 300–800 nm were shown in Fig S1a and b (ESI†), and there was no absorption and emission peaks showed up. The transmittance of PAAS WAR/microemulsion system has been characterized in Fig S1c.† The corrections have been applied to estimate the effect of the light loss in PAAS WAR/microemulsion system (details in ESI†). Relationship of TTA-UC intensity and excitation light power density had been explored in Fig. 3. The intensity of WAR UC materials enhanced as the increase of excitation light power density (Fig. 3a). Fig. 3b showed logarithmic plot of TTA-UC intensity *versus* excitation light power

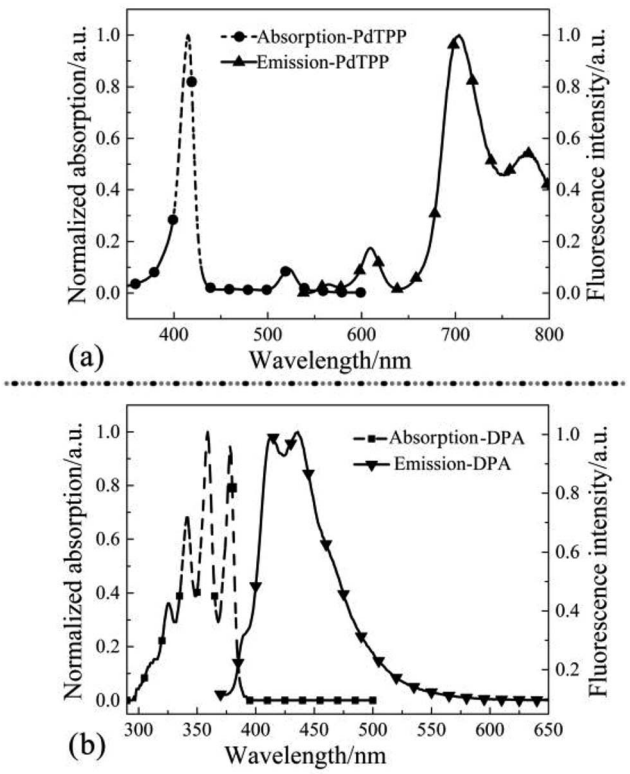

Fig. 1 Absorption and fluorescence spectra of PdTPP (a) and DPA (b) with solvent toluene at a concentration of 1×10^{-6} mol L^{-1}.

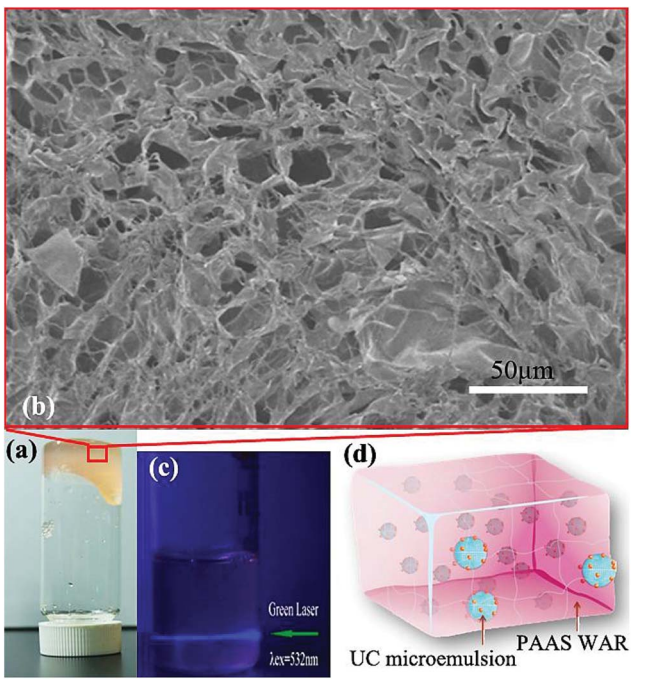

Fig. 2 (a) Photograph of WAR UC materials; (b) microstructure of WAR UC materials; (c) photograph of UC fluorescence of WAR materials; (d) schematic diagram of UC microemulsion in microcellular of WAR UC materials.

Open Access Article. Published on 05 June 2019. Downloaded on 12/9/2025 5:39:30 PM.
This article is licensed under a Creative Commons Attribution-NonCommercial 3.0 Unported Licence.

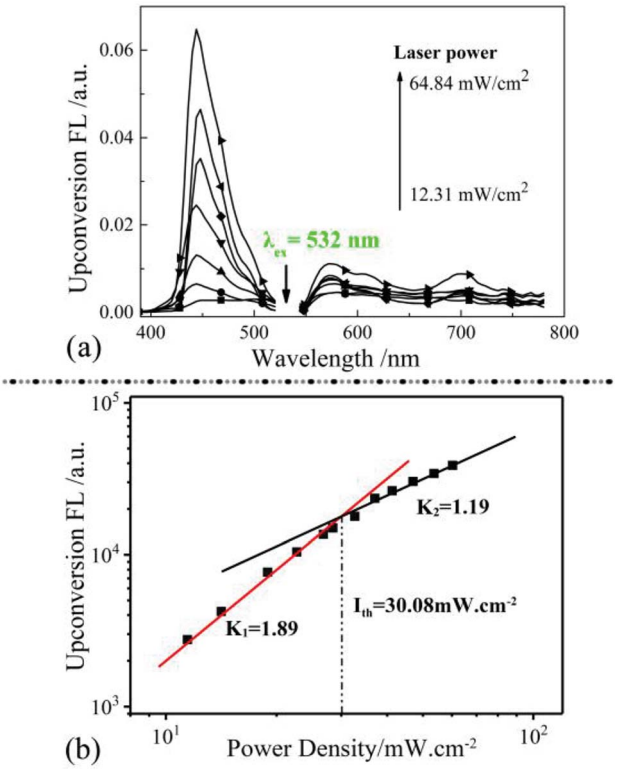

Fig. 3 (a) Spectrum of UC intensity under different excitation light power density of WAR UC materials; (b) logarithmic plots of upconversion intensity *versus* excitation light power density of WAR UC materials.

density from 11.45 mW cm^{-2} to 30.08 mW cm^{-2}, and the obtained K_1 value is 1.89 that closed to 2. The value represents two photons absorption of the TTA-UC process and the maximum efficiency has been reached. When the excitation light power density were increased from 30.08 mW cm^{-2} to 60.3 mW cm^{-2}, the obtained K_2 value is 1.19 that closed to 1. The value of 1.19 suggests that the two photons absorption process has achieved a saturated situation and efficiency attenuation of the TTA-UC process may occur.[39] Thus, the excitation power in our upconversion measurements should be limited below 30.08 mW cm^{-2}. The relationship of the WAR UC materials was the same as UC in solution system, which indicated that the PAAS resin could provide analogous condition for TTA-UC as solution system. The efficiency of WAR UC under different temperature has been studied in Fig. S2 (ESI†).

Conventional methods for the production of 7-hydroxycoumarin may cause formation of by-products and introduces corrosion problems. For these reasons, some attempts should be taken to find alternative environmentally benign and heterogeneously catalyzed synthesis routes.[40] The TTA-based upconversion can be obtained at very low excitation energy and even near-infrared light, which has a much higher penetration depth through various media, notably biological tissue.[41] TTA-UC has the ability to transform the unused low energy radiation into high energy photons that beyond energy gaps of main commercial photocatalysts, and consequently trigger the chemical synthesis, which shows potential applications in photovoltaics and photocatalysis. Here, the WAR UC materials was firstly used to drive photocatalytic synthesis of organic molecules in air. Photocatalytic synthesis is a technology that using illuminant as a chemical synthesis element to substitute chemical reagent or synthesis condition, which supplied an environmentally friendly way for conventional chemical synthesis.[42]

In this paper, WAR UC fluorescence was used as illuminant for the photocatalytic synthesis of 7-hydroxycoumarin using coumarin as raw material. Emission characteristic peaks of coumarin and 7-hydroxycoumarin were at 375 nm and 460 nm as shown in Fig. 4a. The initial concentration of coumarin is two orders of magnitude larger than 7-hydroxycoumarin, which made the spectra intensity of coumarin is nearly constant as shown in Fig. 4a. There was no fluorescence peak at 460 nm at the beginning, while this fluorescence peak increased as illumination time increasing. This phenomenon demonstrated that 7-hydroxycoumarin was generated though the photocatalytic synthesis, and its concentration in solution was increasing as the illumination of WAR UC fluorescence continued. The photocatalytic synthesis of 7-hydroxycoumarin

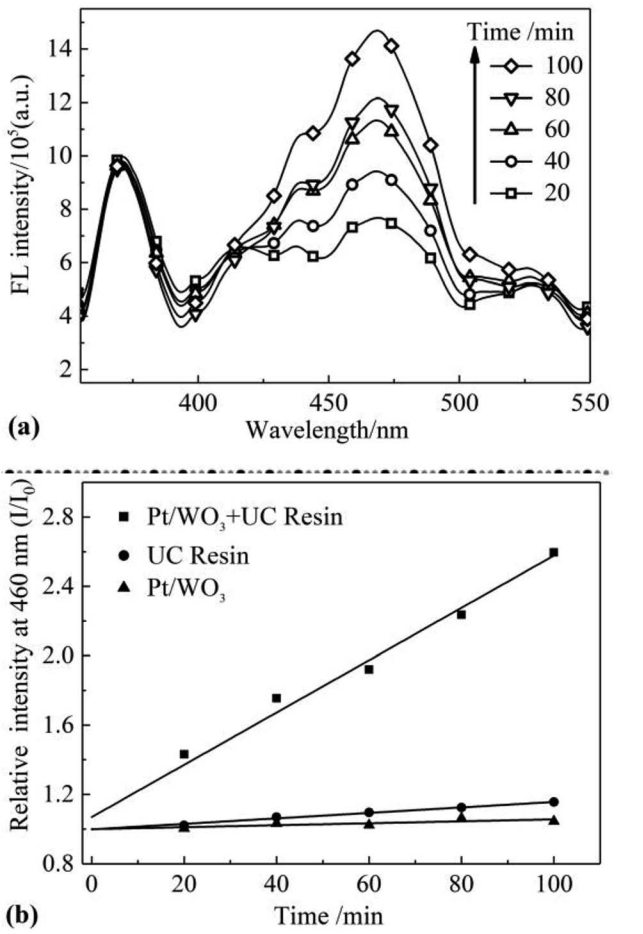

Fig. 4 (a) Fluorescence spectrum of 7-hydroxycoumarin under different irradiation time; (b) conversion rate of coumarin under different conditions.

This journal is © The Royal Society of Chemistry 2019

Open Access Article. Published on 05 June 2019. Downloaded on 12/9/2025 5:39:30 PM.
This article is licensed under a Creative Commons Attribution-NonCommercial 3.0 Unported Licence.

needed a short time to be stable at the beginning. Peaks at 413 nm and 435 nm were characteristic peaks of DPA. The vast majority of the DPA was encapsulated into the PAAS resin along with microemulsion. However, there remained small amount of the DPA molecules in the outermost layer of PAAS resin, which could diffuse into coumarin solution. Emission spectra of DPA and 7-hydroxycoumarin tested using laser (365 nm) was shown in Fig. S3 (ESI†). The spectra intensity of DPA at 420 nm came closer to the constant after 20 min, suggesting the concentration of DPA in solution had already balanced. And the effect of DPA could be considered as the same because the spectra intensity of DPA was constant all along the photocatalytic synthesis of 7-hydroxycoumarin (Fig. 4a).

The mechanism of the photocatalytic synthesis was as follow: Firstly, low energy green light was converted into blue light of high energy that matched the band gap of Pt/WO_3. Then electrons of Pt/WO_3 was excited and transferred from valence band to conduction band. Secondly, the electrons on conduction band reacted with dissolved oxygen in solution and generated superoxide anion and hydroxyl radical.[43] The hydroxyl radical on Pt/WO_3 is mainly generated through the reduction of O_2. The charge carriers on conduction band reacted with dissolved oxygen in solution and generated $\cdot O_2^-$ radical. Then H_2O_2 was generated by the reaction between $\cdot O_2^-$ radical and H^+. And H_2O_2 was reduced by electrons and splited into hydroxyl radical and OH^-. The electron of OH^- can be despoiled by electron hole and also transferred into hydroxyl radical. The reaction equations (eqn (S13)–(S20)) are shown in ESI.† Coumarin combined with the hydroxyl radical and converted into 7-hydroxycoumarin.

Single factor groups of photocatalyst and UC fluorescence were established to determine the dominant factor. Under the same condition, one group without WAR while the other without Pt/WO_3 (Fig. 4b). The ratio of fluorescence intensity of 7-hydroxycoumarin over time and the initial intensity (I/I_0) was calculated as conversion rate. As seen in Fig. 4b, the conversion rates of 7-hydroxycoumarin in the two single factor groups were nearly constant. While only the two factors of photocatalyst and UC fluorescence coexisted, the conversion rates of 7-hydroxycoumarin increased and was proportional to time. The efficiency of photocatalytic synthesis of 7-hydroxycoumarin was also obtained (eqn (S12), ESI†).

Another demo application of WAR UC materials in the photocatalytic degradation were demonstrated. Rhodamine B is a mature industrial dye that has been widely applied in cosmetics and colored glass field. However, rhodamine B is carcinogenic and its industrial or domestic waste may be threats for human health. Using the UC fluorescence as illuminant, we tried to study the photocatalyst degradation behavior of rhodamine B by WAR UC materials. Schematic diagram of the photocatalytic degradation of rhodamine B was shown in Fig. 5a. Semiconductor materials ZnCdS was used as photocatalyst. Under the irradiation of 532 nm laser, PdTPP and DPA emitted high-energy UC fluorescence that exciting ZnCdS to generate electric charge effect. Through the electric charge effect, rhodamine B was gradually degraded.

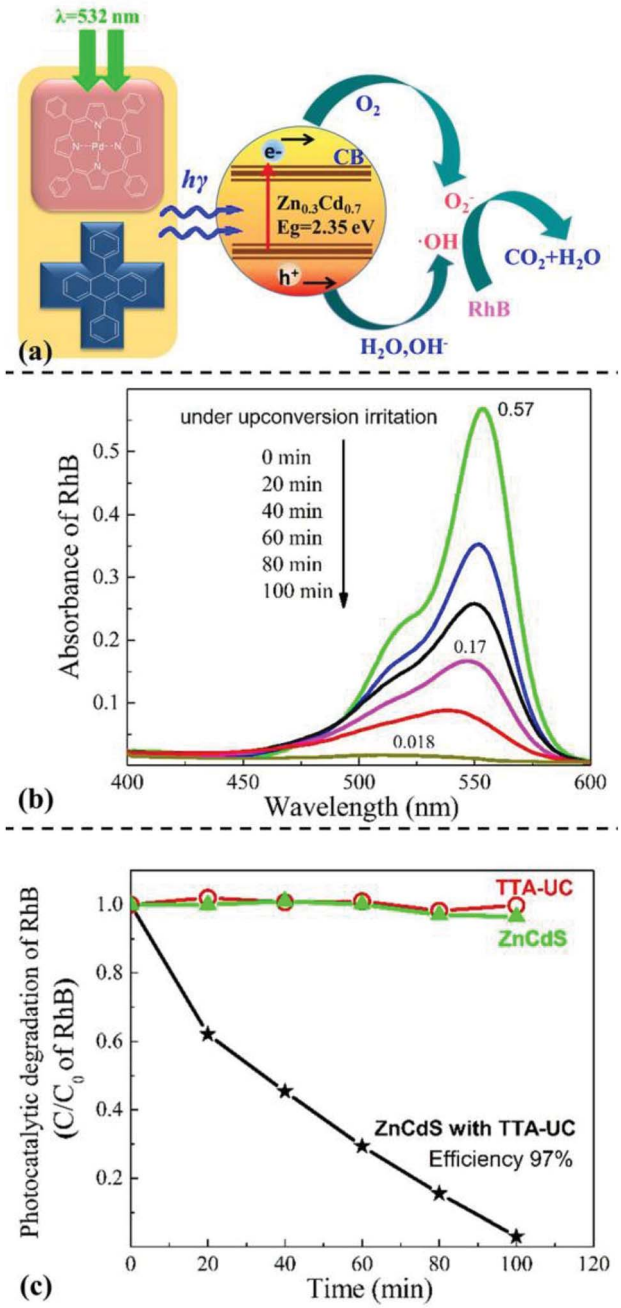

Fig. 5 (a) Schematic diagram of photo-degradation test of WAR UC materials/ZnCdS/rhodamine B; (b) absorption fluorescence spectra of rhodamine B under different irradiation time; (c) photo-degradation curves of rhodamine B under different conditions.

Absorption spectrum of rhodamine B solution varied over time under the irradiation of WAR UC fluorescence as shown in Fig. 5b. Absorbance intensity of rhodamine B gradually declined along with the irradiation of UC fluorescence, which means the concentration of rhodamine B declined gradually. The initial absorbance of rhodamine B was 0.57, while the value turned to 0.018 after illumination for 10 min. The concentration of rhodamine B had decreased for almost 97%, which indicated

Open Access Article. Published on 05 June 2019. Downloaded on 12/9/2025 5:39:30 PM.
This article is licensed under a Creative Commons Attribution-NonCommercial 3.0 Unported Licence.

a remarkable photocatalytic degradation of rhodamine B through WAR UC materials.

Single factor groups of photocatalyst and UC fluorescence were also established to determine the dominant factor. Under the same condition, one group without WAR while the other without ZnCdS, as shown in Fig. 5c. The relative concentration of rhodamine B in the two single factor groups were nearly constant. While only the two factors of photo catalyst and UC fluorescence coexisted, the relative concentration of rhodamine B decreased distinctly over time. The degradation efficiency was up to 97% that corresponded to the result of ultraviolet absorption test. The mechanism of the degradation of rhodamine B was as follows. Firstly, low energy exciting light was converted into blue UC fluorescence of high energy through WAR. Secondly, the energy of blue UC fluorescence beyond the energy difference of valence band and conduction band of ZnCdS, which generated electron holes and electrons. And these charge carriers on conduction band reacted with dissolved oxygen in solution and generated hydroxyl radical in the same way of Pt/WO_3. The reaction equations are shown in ESI.† Thirdly, rhodamine B was gradually degraded into CO_2 and H_2O by hydroxyl radical following a series of redox processes. The remarkable photocatalytic degradation of rhodamine B through WAR material demonstrated the potential in industrial applications of photocatalytic degradation field.

4 Conclusions

In this paper, water-absorbent resin (WAR) solid-state upconversion (UC) material based on triplet–triplet annihilation mechanism was prepared by loading PdTPP/DPA as sensitizers and annihilators, using polyporous sodium polyacrylate as matrix. PdTPP/DPA was dissolved in toluene and prepared into O/W microemulsion. Characterization of micro-morphology revealed that porous microstructures of the PAAS resin absorbed the microemulsion to form WAR UC materials. UC property showed that PAAS WAR UC materials revealed strong blue emission under the simulation of a semiconductor laser (532 nm, 60 mW cm^{-2}), realizing highly efficient solid-state TTA-UC in air. In the further application measurement, photocatalyst Pt/WO_3 was excited by UC emission from WAR UC materials to produce hydroxyl radicals, yielding 7-hydroxycoumarin by reacted with coumarin. Similarly, the band gap of ZnCdS matched the energy of UC emission, hole–electron pairs were obtained under the UC irradiation and captured electrons from rhodamine B, leading to the degradation of rhodamine B. The maximum photocatalysis efficiency was up to 97%.

This work solves the oxygen quenching problem and opens a new avenue to solid-state devices for TTA-UC by the prepared WAR UC materials. Furthermore, the applications of photocatalytic synthesis and photocatalytic degradation lay a foundation for future practical applications for TTA-UC materials.

Conflicts of interest

There are no conflicts to declare.

Acknowledgements

The authors are grateful to National Natural Science Foundation of China (Grant No. 51873145, 51603141), Natural Science Foundation of Jiangsu Province-Excellent Youth Foundation (BK20170065), Natural Science Foundation of Jiangsu Province (BK20160358), Natural Science Foundation of the Higher Education Institutions of Jiangsu Province (17KJA430016), Qing Lan Project, 5th 333 High-level Talents Training Project of Jiangsu Province (No. BRA2018340), Six Talent Summits Project of Jiangsu Province (No. XCL-79) for the financial supports.

References

1 S. L. Chen, J. Stehr, N. K. Reddy, C. W. Tu, W. M. Chen and I. A. Buyanova, *Appl. Phys. B: Lasers Opt.*, 2012, **108**, 919.
2 W. Dong, G. Zhou, X. Xu, X. Wang, Z. Liu, R. Yan, Z. Shao and M. Jiang, *Opt. Laser Technol.*, 2002, **34**, 55.
3 Z. Hasan, L. Biyikli, M. J. Sellars, G. A. Khodaparast, F. S. Richardson and J. R. Quagliano, *Phys. Rev. B: Condens. Matter Mater. Phys.*, 1997, **56**, 4518.
4 C. Ye, L. Zhou, X. Wang and Z. Liang, *Phys. Chem. Chem. Phys.*, 2016, **18**, 10818.
5 W. Bao, B. Sun, X. Wang, C. Ye, D. Ping, Z. Liang, Z. Chen, X. Tao and L. Wu, *J. Phys. Chem. C*, 2014, **118**, 1417.
6 X. Ming, X. Zou, Q. Su, Y. Wei, C. Cong, Q. Wang, X. Zhu, F. Wei and F. Li, *Nat. Commun.*, 2018, **9**, 2698.
7 Q. Dou, L. Jiang, D. Kai, C. Owh and J. L. Xian, *Drug Discovery Today*, 2017, **22**, 1400.
8 Y. T. Liang, B. K. Vijayan, K. A. Gray and M. C. Hersam, *Nano Lett.*, 2011, **11**, 2865.
9 W. Fan, H. Bai and W. Shi, *CrystEngComm*, 2014, **16**, 3059.
10 Y. Yi, L. Cheng, M. Ping and L. J. Wang, *J. Nanomater.*, 2013, **2013**, 13.
11 Y. Chen, J. Zhao, L. Xie, H. Guo and Q. Li, *RSC Adv.*, 2012, **2**, 3942.
12 T. Jing, Y. Ni, C. Lu, C. Jie, Y. Yuan, J. Chen and Z. Xu, *RSC Adv.*, 2014, **4**, 39316.
13 N. M. Idris, M. K. Gnanasammandhan, J. Zhang, P. C. Ho, R. Mahendran and Y. Zhang, *Nat. Med.*, 2012, **18**, 1580.
14 C. Wang, L. Cheng, Y. Liu, X. Wang, X. Ma, Z. Deng, Y. Li and Z. Liu, *Adv. Funct. Mater.*, 2013, **23**, 3077.
15 H. Ling, Y. Zhao, H. Zhang, K. Huang, J. Yang and G. Han, *Angew. Chem., Int. Ed. Engl.*, 2017, **56**, 14400.
16 T. Miteva, V. Yakutkin, G. Nelles and S. Baluschev, *New J. Phys.*, 2008, **10**, 103002.
17 C. Ye, J. Wang, X. Wang, P. Ding, Z. Liang and X. Tao, *Phys. Chem. Chem. Phys.*, 2016, **18**, 3430.
18 K. Xu, J. Zhao and E. G. Moore, *J. Phys. Chem. C*, 2015, **121**, 22665.
19 D. Liu, Y. Zhao, Z. Wang, K. Xu and J. Zhao, *Dalton Trans.*, 2018, **47**, 8619.
20 Q. Li, C. Zhang, J. Y. Zheng, Y. S. Zhao and J. Yao, *Chem. Commun.*, 2011, **48**, 85.
21 K. Xu, Z. Mahmood, D. Escudero, J. Zhao and D. Jacquemin, *J. Phys. Chem. C*, 2015, **119**, 23801.

 This journal is © The Royal Society of Chemistry 2019

Open Access Article. Published on 05 June 2019. Downloaded on 12/9/2025 5:39:30 PM.
This article is licensed under a Creative Commons Attribution-NonCommercial 3.0 Unported Licence.

22 T. Yang, Y. Sun, Q. Liu, W. Feng, P. Yang and F. Li, *Biomaterials*, 2012, **33**, 3733.
23 Z. Mahmood, A. Toffoletti, J. Zhao and A. Barbon, *J. Lumin.*, 2017, **183**, 507.
24 H. Sternlicht, G. C. Nieman and G. W. Robinson, *J. Chem. Phys.*, 1963, **38**, 1326.
25 D. Dzebo, K. Mothpoulsen and B. Albinsson, *Photochem. Photobiol. Sci.*, 2017, **16**, 1327.
26 Z. Xiang, S. Shikha and Z. Yong, *Nanoscale*, 2018, **10**, 16447.
27 S. H. C. Askes, V. C. Leeuwenburgh, W. Pomp, H. Arjmanditash, S. Tanase, T. Schmidt and S. Bonnet, *ACS Biomater. Sci. Eng.*, 2017, **3**, 322.
28 C. Ye, B. Wang, X. Wang, P. Ding, X. Tao, Z. Chen, Z. Liang and Y. Zhou, *J. Mater. Chem. C*, 2014, **2**, 8507.
29 X. Jiang, X. Guo, J. Peng, D. Zhao and Y. Ma, *ACS Appl. Mater. Interfaces*, 2016, **8**, 11441.
30 Y. Y. Cheng, A. Nattestad, T. F. Schulze, R. W. Macqueen, B. Fückel, K. Lips, G. G. Wallace, T. Khoury, M. J. Crossley and T. W. Schmidt, *Chem. Sci.*, 2015, **7**, 559.
31 H. Yonemura, Y. Naka, M. Nishino, H. Sakaguchi and S. Yamada, *Mol. Cryst. Liq. Cryst.*, 2017, **654**, 196.
32 S. Baluschev, P. E. Keivanidis, G. Wegner, J. Jacob, A. C. Grimsdale, K. Mullen, T. Miteva, A. Yasuda and G. Nelles, *Appl. Phys. Lett.*, 2005, **86**, 3065.
33 P. B. Merkel and J. P. Dinnocenzo, *J. Lumin.*, 2009, **129**, 303.
34 L. Li, Y. Zeng, T. Yu, J. Chen, G. Yang and Y. Li, *Chemsuschem*, 2017, **10**, 4610.
35 R. Vadrucci, A. Monguzzi, F. Saenz, B. D. Wilts, Y. C. Simon and C. Weder, *Adv. Mater.*, 2017, **29**, 1702992.
36 L. Nienhaus, M. Wu, V. Bulovia, M. A. Baldo and M. G. Bawendi, *Dalton Trans.*, 2018, **47**, 8509.
37 R. Salhi and J. L. Deschanvres, *J. Lumin.*, 2016, **176**, 250.
38 K. S. Kulkarin, D. Winkler, H. P. Borse and R. Fink, *Appl. Surf. Sci.*, 2001, **169**, 438.
39 A. Haefele, J. Blumhoff, R. S. Khnayzer, *et al.*, *J. Phys. Chem. Lett.*, 2012, **3**, 299.
40 M. C. Laufer, H. Hausmann and W. F. Hölderich, *J. Catal.*, 2003, **218**, 315.
41 D. Benjamin Ravetz, B. P. Andrew, M. C. Emily, *et al.*, *Nature*, 2019, 343.
42 H. Kim, S. Weon, H. Kang, A. L. Hagstrom, O. S. Kwon, Y. S. Lee, W. Choi and J. H. Kim, *Environ. Sci. Technol.*, 2016, **50**, 11184.
43 J. Kim, C. W. Lee and W. Choi, *Environ. Sci. Technol.*, 2010, **44**, 6849.